Article

Riboflavin and Eosin Y Supported on Chromatographic Silica Gel as Heterogeneous Photocatalysts

Daniel A. Caminos,* Guido N. Rimondino, Eduardo Gatica, Walter A. Massad, and Juan E. Argüello*

Cite This: *ACS Omega* 2023, 8, 30705−30715

Read Online

ACCESS | Metrics & More | Article Recommendations | Supporting Information

ABSTRACT: The application of photocatalysis for organic synthesis, both in the laboratory and on an industrial scale, will depend on the achieving of good yields and the ease with which it can be applied. Selective irradiation of the photocatalyst with LED light has made it possible to activate the reactions easily, without the need for UV or heat filters. However, a common problem is the need to separate the photocatalyst from the reaction products through extraction and chromatography isolation processes. These procedures make it difficult to recover and reuse the catalyst, which is not compatible with scale-up applications. Photocatalysts attached to heterogeneous supports resulted in an alternative, which facilitates their removal and reuse. In this study, we use chromatographic silica gel as a low-cost heterogeneous support to bind photosensitizers such as Riboflavin or Eosin Y. The modified silica gel was analyzed by FTIR-ATR and diffuse reflectance UV−visible spectroscopy, thermogravimetric analysis, and optical microscopy. These hybrid materials have a suitable size for easy separation by decantation and were found to be photoactive against two photooxidation reactions. These easy-to-handle materials open the door to effective applications for photoinduced organic synthesis methods at medium to large scale.
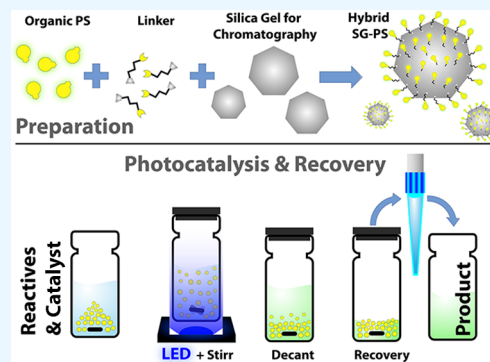
INTRODUCTION

Currently, most of the chemical products on the market require catalysts at some stage in their production. For this reason, and to reduce the environmental impact, the search for more efficient and environmentally friendly catalysts is critical.[1] Photocatalysis has become an emerging and cutting-edge field in organic synthesis. This catalysis is an attractive alternative to perform oxidations, reductions, and C−C and C−Heteroatom bond formation under mild reaction conditions using visible light as a sustainable and low-cost energy source.[2] These catalytic processes involve excited states that allow the transfer of energy (photosensitization) or electrons (photo-redox).[3,4] Many of the photocatalysts studied are based on transition metal complexes (e.g.: Ir and Ru);[2c] however, they are potentially toxic and rare elements, and their use raises costs and limits their application, hindering sustainability and scale-up applications. Alternatively, the use of organic molecules with photochemical activity has advantages.[5] They are cost-efficient, less toxic, and their physicochemical properties can be easily modified compared to transition metal complexes.[5] However, a common drawback is the need for additional isolation steps to separate the products and recover the catalyst. Therefore, work up steps and isolation becomes a time demanding procedures in homogenous photocatalytic protocols. To overcome this, the use of heterogeneous macroscopic catalyst materials allows the separation and reuse the catalyst using simple laboratory techniques.

Recently, our group has focused on photocatalysis in organic synthesis, its reaction mechanisms, and possible platforms to apply this process.[6] Different photocatalysts "based on" or coupled to nanoparticles (NPs) have been tested. However, the construction, characterization, reproducibility, and recovery of these nano-systems have been difficult, expensive, and time-consuming. The nanostructures have low stability and require ultracentrifugation for their separation. Both issues make it difficult to use and recycle NPs on a laboratory scale, and even transferring their application to large-scale synthesis is not an easy goal to achieve.

We are therefore looking for a catalyst that is easy to build and use at laboratory scale, consisting of organic molecules bound to a granular and inert support platform. There are few examples of macroscopic photocatalysts in the literature. In these examples, an organic photocatalyst is bound to silica matrices,[7] molecular sieves,[8] chitosan,[9] polymers,[10] sponges,[11] cellulose,[12] and cotton fibers,[13] which are easier to separate and adapt for laboratory use. To assemble these systems the photocatalyst is generally attached to a heterogeneous support

through electrostatic,[11a,13−15] hydrophobic-hydrophilic inter-actions,[16,17] or covalent bonds.[7,9,10a,11b,12,18] The binding to the support material is usually achieved with a linker.

An interesting example of a heterogeneous photocatalyst is a thin layer-flavin system from Dongare et al.[19] who report the photooxidation of a family of aromatic hydrocarbons by phosphate flavin mononucleotide surface-bound to metal-oxide films. In addition, König et al. achieved the photooxidation of benzyl alcohols using fluorinated or hydrophobic derivatives of flavin adsorbed on fluorinated (35−70 μm) o reversed-phase silica gel (40−63 μm).[16] In that report good yields of aldehyde formation (45−90%) were achieved for various benzyl alcohols. In both papers, the sensitizers were not covalently attached, and the leaching of the catalyst represents the main drawback. On the other hand, Marin et al. have reported the preparation of silica nanoparticles (420−460 nm) decorated with riboflavin and successfully applied to the photo-degradation of phenolic derivative pollutants in water.[20]

With this in mind, we turn to silica gel for chromatography as a possible heterogeneous support. Chromatographic silica gel is widely available and accessible in almost every laboratory. This $SiO_2 \cdot (H_2O)$ material is well known and has Si−OH groups on its surface, which can be used to bind a linker and a photocatalyst.[21] A wide variety of photocatalysts have been studied on the literature; however, we chose riboflavin and Eosin Y (Scheme 1) because their commercial availability and

Scheme 1. Riboflavin and Eosin Y Structures, and Their AM1 Energetic Minimization 3D Images at Room Temperature (∼300 K)
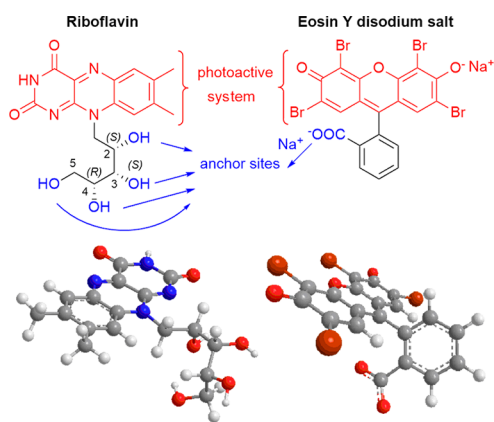
well stablished photochemical properties.[22,23] In addition, their carbon skeleton has appropriate functional groups that allow to bind to a spacer-linker molecule. In our approach, these organic molecules are used to test two grafting techniques on silica gel crystals. We perform a detailed analysis of the construction and characterization of the hybrid material through optical microscopy, UV−visible spectroscopies, FTIR-ATR, and TGA. Then, we complete the studies with chemical tests to evaluate the performance of these photo-catalysts hybrid materials.

■ RESULTS AND DISCUSSION

Silica Gel Properties and Photocatalyst Selection. Many heterogeneous matrices can be considered as support. However, we chose Silica gel 60 (SG), used in chromatography because it is a commercially available material and widely used in laboratories. SG consists mainly of an SiO_2 crystal lattice

(60.08 g/mol) with high and variable water content. This white solid has particles between 0.2−0.5 mm.[24] Silica gel has a slightly acid character given by its Si−OH groups in the outer layer (pH 3.7−4.7) and is therefore sensitive to strong basic media. According to the manufacturer, its solubility in water is 0.076 g/L at 37 °C and its density is 1.430 kg/m^{3}.[20] Generally, SG is considered to be an insoluble solid and unreactive for the reaction conditions used in organic synthesis. Upon observa-tion by optical microscopy, the commercially available solid contains irregularly shaped crystalline particles in its three dimensions (Figure 3a). To establish the size distribution, we adopted the criterion of measuring an average 2D diagonal in ∼800 particles (See SI, page S14). We observed that most SG particles have sizes between 0.06 and 0.2 mm and are transparent to light. The observed white color at the macroscopic level is due to internal scattering. Although the manufacturer indicates a melting point of 1713 °C for SG, our thermo-gravimetric analysis (TGA) showed that silica gel has between 5 and 10% of adsorbed water, which is easily lost at 100 °C, and the crystallization water is lost between 250−800 °C temperature. Then, all these characteristics make silica gel a suitable support for photocatalysis. The particles are large enough to allow their separation by simple laboratory techniques such as filtration, centrifugation, or decantation. Reactions for covalent attachment of dyes to supports typically require multiple wash steps, which can result in the loss of a significant amount of the desired material. In a comparative test, simple decantation was found to be the best washing and recovery method for silica gel chromatography (See SI, page S3).

As mentioned above, Riboflavin (RF) and Eosin Y (Eo) were chosen as photocatalysts. However, each compound requires different anchoring techniques. Both photosensitizers have a chromophore group which is responsible for their photochemical properties. (Scheme 1). Likewise, the mole-cules have other functional groups that allow them to attach to other molecules. RF has a ribityl side chain that gives the flavin chromophore freedom of movement. Using unmodified RF, four hydroxyl groups can serve as an anchor site. In particular, the HO group on the primary carbon is expected to be the most reactive.[25] However, it makes no difference to the system whether the anchor occurs in the other secondary HO groups, at least for photocatalyst purposes. Since we expect that, the flavin will have freedom of movement in all cases (See SI, page S4). Besides, Eo has a more rigid skeleton, its $-C_6H_4-COO^-$ group is perpendicular to the chromophore. For Eo, (3-aminopropyl)triethoxysilane (APTES) is selected as the linker that attaches the Eo to the SG resulting in a lesser rigid hybrid material.

Silica Gel Grafting. Two different grafting methods were used to modify the SG surface, both of which require stirring where the silica particles can suffer collision and erosion effects. Therefore, to reduce these effects, magnetic stirring was kept to a minimum r.p.m. Subsequently, both grafting methods require many washing and decanting cycles (See Methods section) and UV−visible spectroscopy was used to monitor the complete removal of the unbound dye (Rf or Eo) on the SG. However, this method does not allow the quantification of the dye bound to the SG. Thermogravimetric analysis (TGA), attenuated total reflectance infrared spectra (FTIR-ATR) and diffuse reflectance spectroscopy methods were then used to characterize the hybrid material. In both cases, modified silica gel was obtained. These hybrid materials can be separated by

simple decantation and possess fluorescence due to the attached photosensitizer (Figure 1).
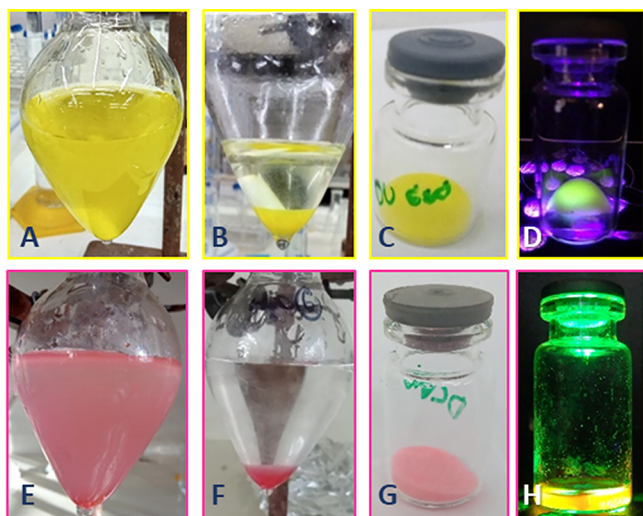

Figure 1. Chromatographic silica gel modified with RF (up panels) or Eosin Y (bottom panels). From left to right, hybrid material re-suspended in water (A, E), after decanting (B, F) and the recovered solid (C, G). Finally, the hybrid material with RF is seen under the light of 395 nm (D), or for Eo, under Green LED (517 nm) in DMF.
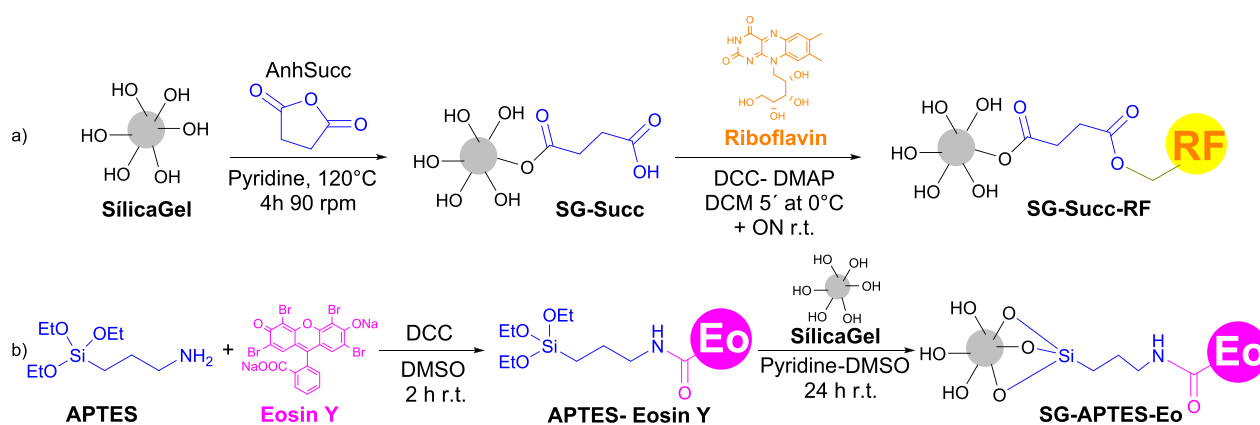
RF Attach to Modified Silica Gel. A two-step strategy was used to bind the commercially available RF. First, succinic anhydride binds to the SG surface to form an ester group using refluxing pyridine as a solvent for 4 h. The pyridine activates the silica surface for ester formation. The pyridine solution was then removed, and the solid was washed with water, ethanol, and acetone. Finally, the modified SG-Succ was dried (See SI page S5). This succinic linker thus binds to SG, leaving a free COOH group to anchor the RF through the HO groups in the ribityl side chain in a second step-pot. (Scheme 2a). Afterward, the new ester bond formation was promoted by a carbodiimide (DCC) and dimethyl amino pyridine (DMAP) as the base. The same reaction was performed in DMSO, DMF, and DCM. Even though DMSO and DMF dissolve RF better than DCM, the coupling reaction gave better results with DCM, giving yellow-colored silica. With DMSO and DMF, the RF remains in the solution and does not bind to the SG-Succ. (See SI, page S8). In this reaction there are two solid phases: the SG modified with RF (SG-Succ-RF) and the dicyclohexyl urea residue generated by the DCC coupling. While the SG-Succ-RF precipitates, the urea residue remains at the upper layer of the solvent, and it was removed in the first washes. After extensive washing steps with DMF, water, ethanol, and acetone, SG-Succ-RF was oven dried. (Figure 1, up panels).

Eosyin Y Attach to Silica Gel with APTES. A classical method of silica modification was used to bind Eosin Y.[26,27] In the first step, Eosin Y and APTES linker react in a 10 mL vial using DCC in DMSO (Scheme 2b). This mixture reacts for two hours and is then transferred to a conical flask containing SG suspended in 12.5% pyridine/DMSO. Under these conditions, the pyridine activates the silica gel surface to promote the formation of the silane ester bonds with the linker. This reaction was left overnight with gentle stirring. The next day, the hybrid solid was allowed to decant, and then wash/decantation cycles were performed with DMSO, water, ethanol, and acetone, and then oven dried. (Figure 1, bottom panels). Depending on the amount of Eo used in the reaction, different SG-APTES-Eo hybrids were obtained (See SI, page S9).

Hybrid Material Characterization. In order to confirm the covalent bond, several tests and checks were carried out on the hybrid materials. For example, we tried to bind SG using succinic acid as a linker for the first RF binding step. After the second reaction step with RF, only white SG was obtained. The same happens when the DCC coupling agent is not present (See SI, page S8). Similarly, for SG modified with Eosin Y controls where the APTES linker or coupling agents are not added, the silica does not present pink color after the washing steps. These modified SG particles precipitate out of solution, and constant stirring is necessary to keep the dispersion of the hybrid material, a condition in which UV−visible spectrum cannot be recorded. As mentioned above, UV−visible spectroscopy was used to determine the presence of unbound dye, but this technique is not accurate enough to establish the amount of bound dye to SG (See SI, pages S7 for RF and S9 for Eo).

Scheme 2. Reactions for Surface Modification of Silica Gel for Chromatography[a]

[a](a) A succinic linker is attached to the silica gel in the first step. In the second step, SG−Succ reacts with riboflavin to give the hybrid material SG−Succ−RF. (b) The Eosin Y disodium salt reacts with APTES to form an amide using DCC. In a second step, the APTES−Eosin product was transferred to a second−round flask and reacted with the silica gel, pre−activated with pyridine in DMSO to obtain the SG−APTES−Eo.
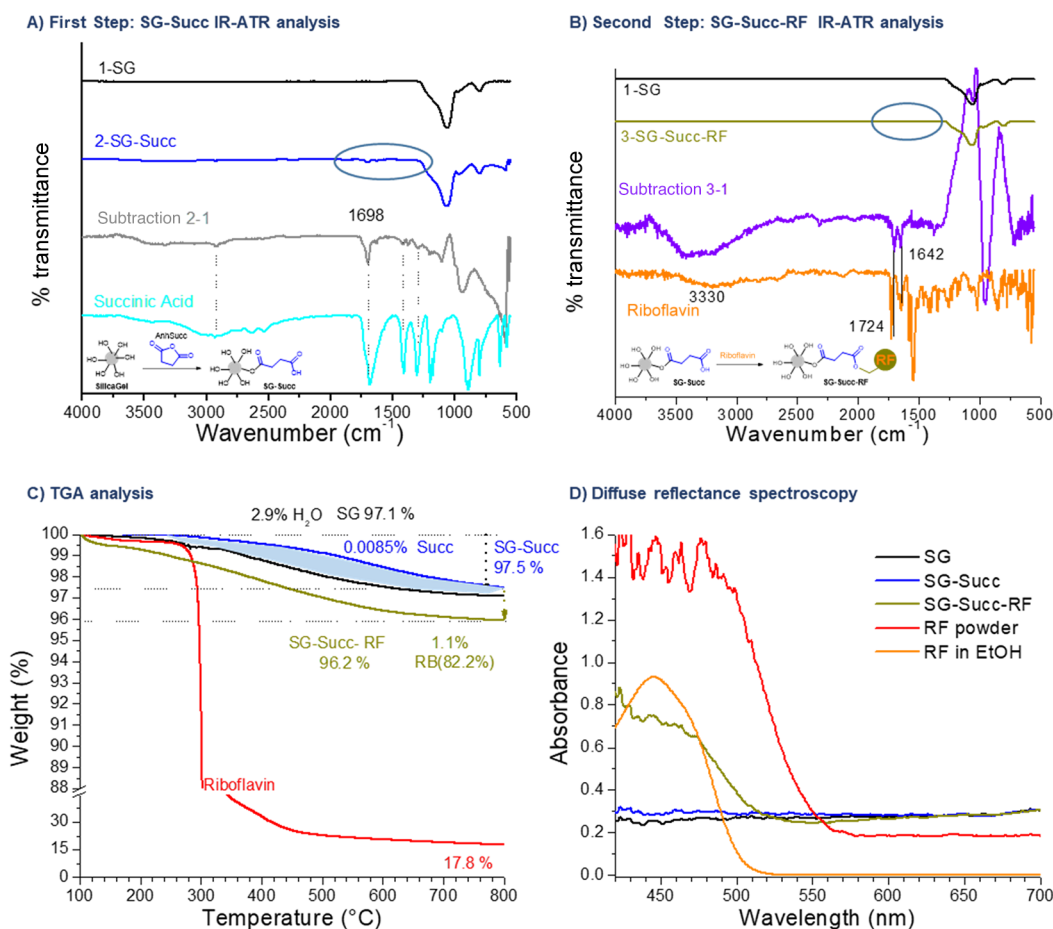
Figure 2. Analysis for modified SG with RF and a Succinic linker. (A) FTIR-ATRs of the SG-Succ. The detailed analysis of the spectra subtraction present signals that suggest the presence of the Si-O-CO-CH$_2$-CH$_2$-COOH residue. (B) FTIR-ATRs of SG-Succ-RF and the spectra subtraction showing RF signals. (C) TGA analysis for both "dry" SG (black), SG-Succ (blue), SG-Succ-RF (dark yellow), and riboflavin (red). The light blue shadow shows the shape difference due to the presence of the organic linker. (D) Diffuse reflectance spectroscopy at 45° for SG (black), SG-Succ (blue), SG-Succ-RF (dark yellow), and riboflavin powder (red) or riboflavin solution in ethanol (orange).

Therefore, thermos-gravimetric analysis (TGA) was used to determine the composition of the hybrid product. (Figure 2). The succinic linker content in SG-Succ is low and difficult to determine. However, the TGA shape analysis showed significant differences. In the case of SG-Succ, the curve corresponds to the decomposition of the Succ residue, around 500 °C. However, the final weight at 800 °C is similar to that of the SG. These results, therefore, make it difficult to quantify the degree of grafting of the Succinic linker. However, for SG-Succ-RF there is a significant change in both shape and mass at 800 °C, with a loss of 3.8% in weight. A pure RF control experiment shows that the dye decomposes between 250−500 °C, leaving a residue corresponding to 17.8%. Considering both results, we determined that the SG-Succ-RF contains about 0.035 mmol RF/g of hybrid material (See SI, page S11). A similar analysis shows that SG-APTES-Eo contains 3% Eosin by weight, and corresponding to 0.058 mmol of Eo/g (See SI, page S13).

In addition, these materials were characterized by FTIR-ATR spectroscopy and UV−vis diffuse reflectance spectrometry (DRS). In FTIR-ATR analysis, a strong broad absorption band of the Si−O bond at 1100 cm^{-1} hinders the signals of the attached organic compounds. For this reason, digital subtraction of the pure SG spectrum to SG-Succ and SG-Succ-RF spectra was performed to facilitate further spectro-scopic analyses. As shown in Figure 2, the (SG-Succ)-SG subtraction presents a signal at 1690 cm^{-1} attributed to the carbonyl groups (st C=O) of the succinic linker. Similarly, the spectra subtraction for (SG-Succ-RF)-SG show bands assigned to RF between 1700 and 1650 cm^{-1}. A similar behavior was observed for the hybrid materials which combine silica gel and Eosin (See SI, Figure S12). Besides the observable color at the macroscopic level, a reflectance diffuse UV−visible light spectrum of the hybrid material was recorded for further characterization. As can be seen in Figure 2D, dried SG and SG-Succ show no signal, but an increase of 0.3 abs across the visible spectrum. While for RF powder, the absorbance is increases from 565 nm to saturate the detector below 500 nm. On the other hand, SG-Succ-RF presents an increase at 525 nm and a shoulder at 450 nm with 0.6 abs. Thus, the band presented by the SG-Succ-RF differs from the solid RF spectrum but matches with the RF spectrum in ethanol (with a maximum at 450 nm). This effect would indicate that the RF is not present in aggregated form on the surface. The same was observed for SG-APTES-Eosin with a maximum at 525 nm, similar to Eosin Y in solution (See SI, page S13).

Summarizing, the weak IR signals make it difficult to unequivocally confirm the ester or amide bond formation for RF and Eosin Y, respectively. However, the combination of washes monitored by UV−visible, chemical controls, TGA,

FTIR-ATR, and DRS results points to the presence of the covalent bond in these hybrid materials.

In addition to chemical composition and spectroscopic study, the micro-particle morphology was also a significant aspect of the materials to be further explored. As mentioned above, the micrography of the SG starting material is presented in Figure 3a. The changes in the morphology along the grafting
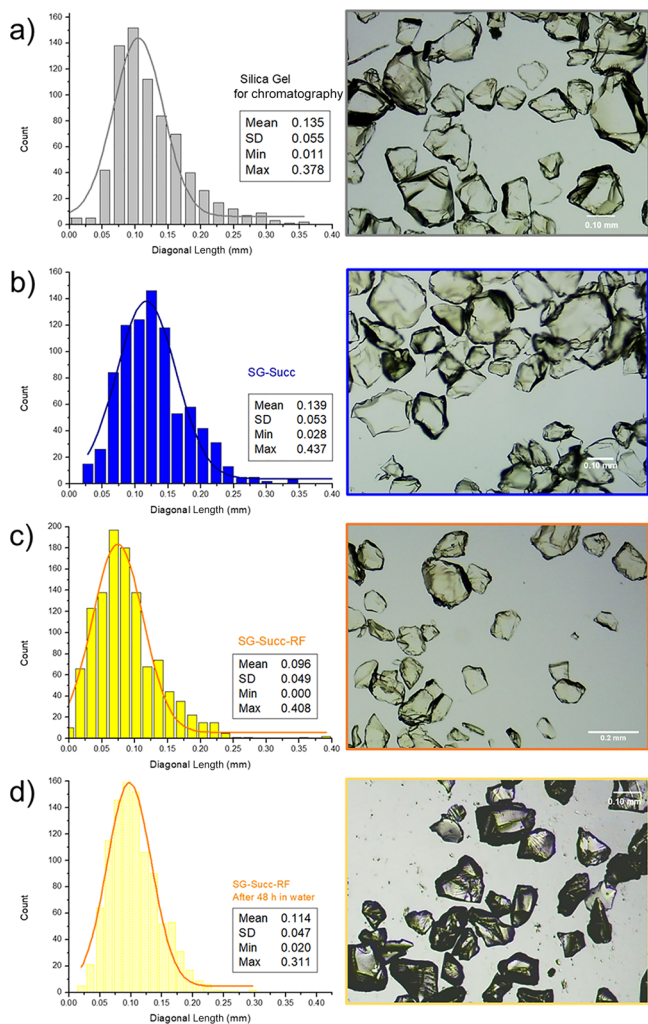

Figure 3. Size distribution histogram of silica gel particles and microscopy images for (a) SG (b) SG-Succ), (c) SG-Succ-RF, and (d) the discolored SG-Succ-RF after incubation in water for 48 h. Note that 800−1000 crystals were counted for the histogram.

process were monitored by microscopy. Thus, after succinic linker binding, which involves 12 washing cycles, the micrographs showed no significant changes in the shape and size of the particles (Figure 3b). Subsequently in the RF binding reaction, which involves several washes with water, a slight variation in the particle size population was observed (Figure 3c). The histograms show a decrease in large particles, and a concomitant increase in small particles, possibly due to erosive beating that reduces the size of particles. A second batch of SG-Succ-RF showed a similar distribution. This second batch was left in water for 48 h to study the RF leaching. After this time, the silica discolors, and the aqueous solution presented an intense yellow color, while micrograph analysis shows no critical changes in shape along this bleaching process (Figure 3d). We attribute this change to the solubility

of SG in water, with the modified SG losing its RF outer layer in strongly polar solvents (See SI, page S16). In the case of SG-APTES-Eo, since its synthesis requires fewer washes, there are no significant differences between the original SG and the dry SG (See SI, page S15).

Photochemical Properties. To evaluate the performance of the modified silica in photochemical reactions, the oxidation of 9,10-dimethylanthracene (DMA) was used as proof of concept. This compound reacts with singlet oxygen to form a 9,10-dimethyl-9,10-dihydro-9,10-epidioxyanthracene endoperoxide (eq 1, **1**) in DMF as solvent. Under the reaction conditions, singlet oxygen is photogenerated by SG-supported RF or Eo dyes under blue or green LED irradiation, respectively.

In our experiment, DMA solution and SG-Succ-RF suspended in DMF are stirred and irradiated at different times. The vial was then removed from irradiation and allowed to decant for 2 min. Then 3 mL were extracted, and the decrease of the 379 nm band of the DMA was measured by UV−Visible spectroscopy (Figure 4). With this procedure, the SG-Succ-RF particles remain in the irradiation vessel. Figure 4, inset B2, shows that RF is absent in the supernatant solution.

Several controls were performed for this study (See SI, page S19). Usually, with this reaction, k_{obs} can be determined by a *pseudo*-first order kinetic equation.[22] Although this curve does not show a linear behavior, the estimated values of the k_{obs} of the SG-Succ-RF are 24 times higher than those of the DMA irradiated with blue light only. Since DMA absorption bands slightly overlap with blue light, its self-bleaching is negligible compared to the SG-Succ-RF composite (See Table 1, and SI pages S19−S23). Furthermore, in the corresponding dark control, DMA is not affected. On the other hand, the presence of SG particles shows a similar behavior to DMA irradiated alone (Figure 4C).

The amount of RF in the SG-Succ-RF composite used was similar to a solution of RF with 0.3 absorbance at $\lambda_{max} = 442$ nm, based on the RF content of the hybrid material determined by TGA. An RF dye solution (0.3 absorbance) decomposes the DMA faster than SG-Succ-RF, but several by-products appear in the solution (See SI, Figure S22). Curiously, even SG-Succ-RF is less photoactive resulted more photostable than homogeneous RF for the same irradiation time. SG-Succ-RF takes about 25 min to bleach, and the discoloration indicates the loss of the chromophore. The same effect was observed with soluble RF at <5 min. Furthermore, a complementary experiment with homogeneous RF 0.005 abs showed that the photocatalytic activity of the SG-Succ-RF does not correspond to an RF release or desorption from the hybrid material (Figure 4C, and SI Figure S23).

The results obtained clearly demonstrate that the hybrid material contributes to the oxidation reaction. It is important to note that photochemistry of this composite does not follow a *pseudo*-first-order mechanism. Since the RF is immobilized on the support, the oxygen must approach to the RF* and then the singlet oxygen migrates in the solution to find the DMA. Under these conditions, the concentration of singlet oxygen in the vicinity of the solid cannot be considered constant. Although the reaction is slower, the advantages of purification are evident. The product can be easily isolated and separated from the catalyst. In addition, typical RF photobleaching by-product spectra were not detected in the solution (See SI, Figure S18).
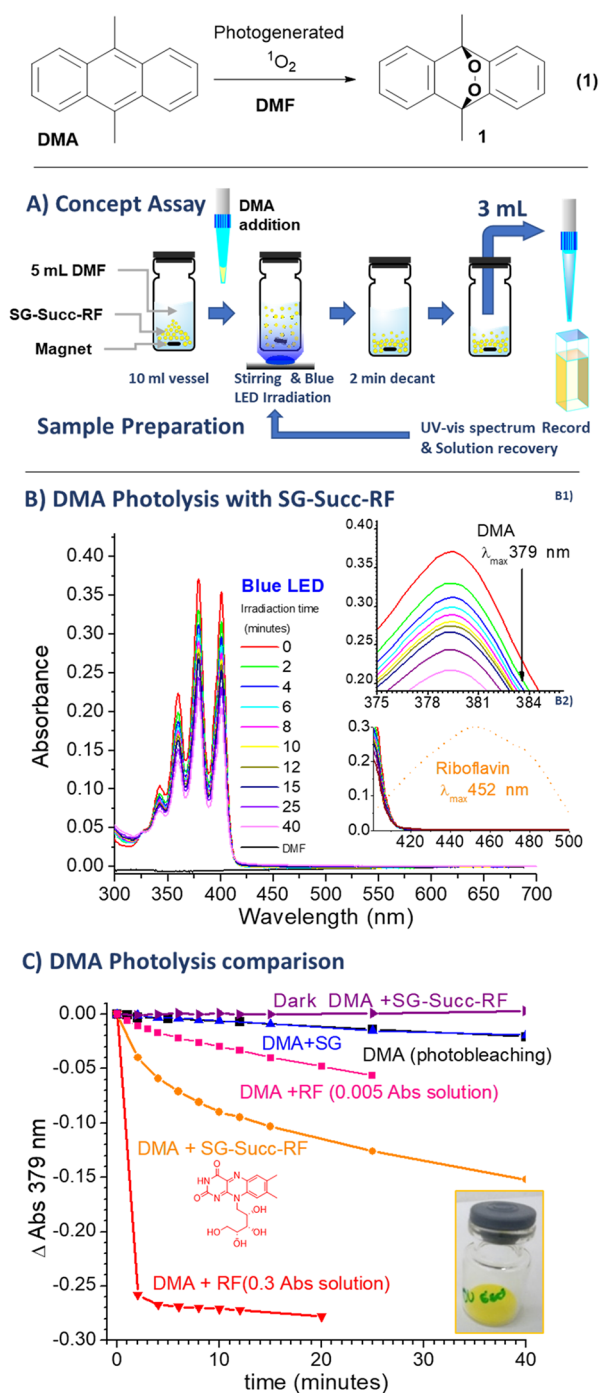
(1)

Table 1. Comparative k_{obs} for DMA Photooxidation

		$\ln (A_0/A_i)$ vs t (s)
sample	*pseudo* 1st order	k_{obs} 10^{-4} s^{-1}
Irradiation Blue LED 3 W-λ_{max} 455 nm		
DMA control	yes	0.234 ± 0.004
SG	yes	0.301 ± 0.004
SG-Succ-RF	no	4.8 ± 0.4
RF solution	no	large
RF 0.005 Abs	no	1.53 ± 0.07
Irradiation Green LED 3 W-λ_{max} 517 nm		
DMA control	yes	0.127 ± 0.002
SG	yes	−0.008 ± 0.01
Eosin Y solution	yes	41.9 ± 0.04
SG-APTES-Eo	no	0.69 ± 0.08

Figure 4. (1) DMA photooxidation with photogenerated singlet oxygen. (A) experimental procedure used in the experiment. (B) DMA photolysis followed by UV−Vis Spectroscopy. In insert B1, the decay of the 379 nm band is shown in detail. In insert B2, in the region close to 452 nm, the presence of soluble Riboflavin released from the hybrid material is not observed. (C) Comparative experiments of the decrease in absorbance (ΔAbs 379 nm) by photosensitization of DMA with SG-Succ-RF under Blue LED irradiation (orange) or in the dark (violet) and compared with RF in solution (Abs 0.3, in red; Abs 0.005 in pink). As an additional control, the photobleaching of DMA under blue light (black) or in the presence of SG alone is shown (blue).

The response of SG-APTES-Eo was also evaluated in a similar experiment. Again, the hybrid material was effective for

DMA oxidation (See Table 1 and SI, page S24). Unlike SG-Succ-RF, SG-APTES-Eo remained colored after the irradiation experiment and could be reused.

To further explore the potential of these materials, the photochemical response of the oxidation of furfuryl alcohol (FFA) in aqueous solution, was considered. The oxygen consumption assay gets more insight into the performance and versatility of these hybrid materials. It is well documented that a Flavin mononucleotide (FMN) solution, when irradiated, can produce $^1O_2$ and $O_2^{\bullet-}$; with quantum yields of 0.49 and 0.009 respectively.[28,29] To confirm the production of $^1O_2$, the O_2-uptake of a FFA solution (0.5 mM) was measured when an aqueous dispersion SG-Succ-RF particles (0.03% w/v, pH = 6) was irradiated at different irradiation times (Figure 5). FFA is a common reference substrate to identify $^1O_2$. Furfuryl alcohol reacts with $^1O_2$ to give 6-hydroxy(2H)pyran-3(6H)-one (eq 2, **2**) as the main product (~85%)[25] with a reactive rate constant, $k_r = 1.2 \times 10^8$ M^{-1} s^{-1}.[30,31]

The results of O_2-uptake measurements upon irradiation of the SG-Succ-RF + FFA system, are shown in Figure 5B and strongly suggest the involvement of radical oxygen species (ROS). To confirm the $^1O_2$ formation by an irradiated suspension of SG-Succ-RF, the same experiment was performed in the absence of FFA. In this case, the rate of O_2-uptake was significantly lower compared to the same solution containing 0.5 mM of FFA. To confirm the $^1O_2$ generation, the O_2-uptake of the SG-Succ-RF + FFA system was also measured in the presence of 2.3 mM NaN$_3$. Anion N$_3^-$ is a physical quencher that deactivates $^1O_2$ with a quenching rate constant of 3×10^8 M^{-1} s^{-1}.[32] However, the quenching of excited RF by azide anion cannot be ruled out, since the quenching rate constant (k_q) for the singlet and triplet exited state of tetra acetylated RF (RFTA) derivative are 5.9 and 7.3×10^9 M^{-1} s^{-1} respectively.[33] As can be observed in Figure 5B, the addition of N$_3^-$ to the SG-Succ-RF + FFA system produces a notable decrease in O_2 consumption. The results of the O_2-uptake experiments evidence the formation of $^1O_2$ when a suspension of SG-Succ-RF is irradiated. This assay confirms that these dyes attached to silica gel are capable of similar photochemistry to the same compound in solution. Yet, as mentioned above, in this test, SG-Succ-RF decolor after irradiation.

The same experiment produces O_2-uptake when SG-APTES-Eo suspension is irradiated in the presence of a 0.5 mM FFA (Figure 5C). The most remarkable difference between the SG-Succ-RF and SG-APTES-Eo systems is that the latter keep their color after the FFA photosensitized
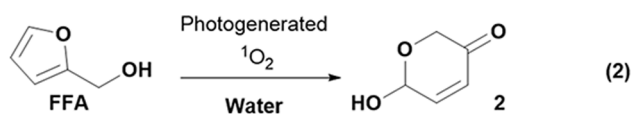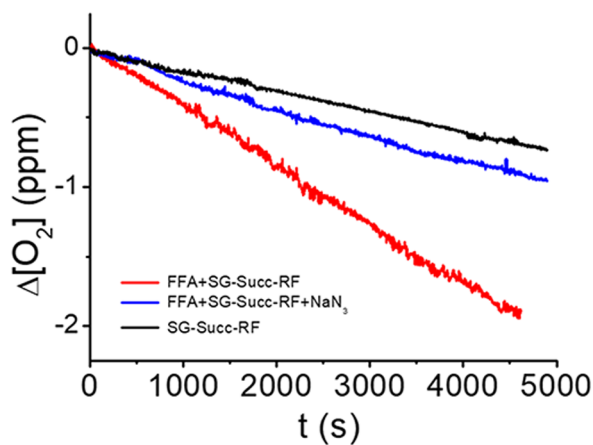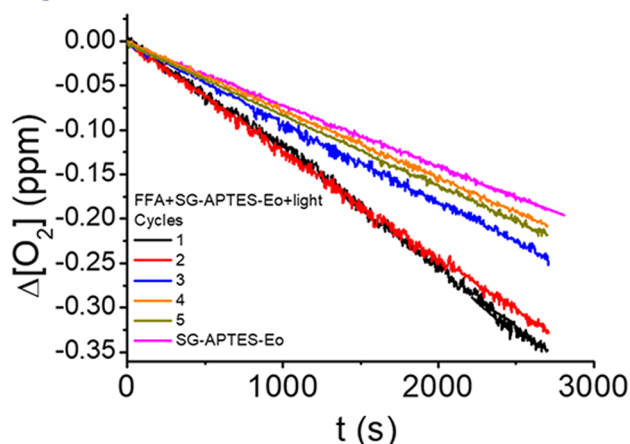
$$FFA \xrightarrow[\text{Water}]{\substack{\text{Photogenerated} \\ {}^1O_2}} 2 \qquad (2)$$

B) O$_2$-uptake at different irradiation time of aqueous suspension

C) O$_2$-uptake cycles with FFA and SG-APTES-Eo

Figure 5. (B) O$_2$-uptake at different irradiation times of aqueous suspensions of: (black line) SG-Succ-RF (0.03% w/v); (red line) SG-Succ-RF (0.03% w/v) + FFA (0.5 mM); and (blue line) SG-Succ-RF (0.03% w/v) + FFA (0.5 mM) + NaN$_3$ (2.3 mM). (C) Number of cycles for which SG-APTES-Eo can be reused at pH 6 plus visible irradiation. 0.5 mM FFA plus SG-APTES-Eo, cycle 1 (black), cycle 2 (red), cycle 3 (blue), cycle 4 (green), cycle 5 (orange). SG-APTES-Eo (magenta).

degradation. In addition, the same FFA assay was employed to study the numbers of reuses for SG-APTES-Eo. Sensitized photolysis experiments were carried out in the water at pH 6, with a suspension of 0.017% w/v of SG-APTES-Eo and 0.5 mM of FFA. Figure 5C shows a pronounced change in slope after two cycles of photolysis (cycles 1 and 2, with a similar slope). For cycles 4 and 5 the slopes indicate no generation of $^1O_2$. Therefore, the FFA is not degraded by the photo process under light irradiation since the oxygen consumption is low. This situation is similar to the photolysis of SG-APTES-Eo without FFA. It's important to mention that the SG-APTES-Eo decolored after the third photolysis cycle. According to our results, we conclude that the SG-APTES-Eo can be recovered and reused up to three photolysis cycles.

Application and Reuse of Silica Gel Modified with Organic Dyes. To evaluate the reusability of these hybrid materials, the reaction of DMA with photogenerated singlet oxygen in DMF was chosen. It is important to note that DMF is not a first option solvent in organic chemical reactions because its removal is difficult. However, we focused our study ass a proof of concept. The modified SG was placed in a 10 mL vessel, and 5 μmol of DMA was added in 3 mL of DMF. In this experiment, 0.1 g of modified SG was used and irradiated with blue or green LED according to the attached dye (RF or Eo). After 1 h of LED irradiation and stirring, the vial was removed from the photoreactor. The reaction is then decanted in the absence of light. The supernatant solution was gently removed and quantified by UV−visible spectroscopy (See SI, page S30). The modified SG was washed with DMF between cycles. A new dose of 5 μmol of DMA in DMF was then added, and the vessel was irradiated for an additional 1 h. Figure 6 shows the
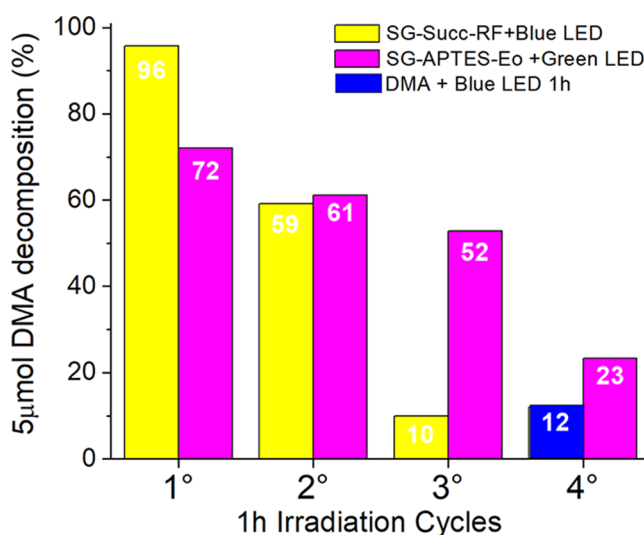

Figure 6. DMA consumption cycles. In each cycle, 5 μmol DMA in 3 mL DMF in the presence of 0.1 g of SG-Succ-RF or SG-APTES-Eo and irradiated for1 h with blue LED or Green LED, respectively.

percentage of DMA consumption after 1 h of irradiation quantified by UV−visible spectroscopy. As shown in the Figure 6, using SG-Succ-RF with blue light (yellow bars), the material was fully active for only one cycle. This low activity corresponds to the noticeable pale yellow discoloration of SG-Succ-RF (See SI, page S17). In the second cycle, the activity of SG-Succ-RF is reduced to half. The remaining activity in the third cycle is attributed to autoxidation of the same DMA with blue LED irradiation, as shown in the control experiment (Figure 6, blue bars). In this case, the RF attached to SG behaves similarly to the RF in the solution; and other immobilized RF.[18] Under our reaction conditions, the RF does not survive irradiation with a 3 W blue LED. On the other hand, when SG-APTES-Eo is used in successive cycles, the material is still active during 3 reaction cycles, (Figure 6, pink bars). These experiments show that the Eosin derivative is less active than RF, yet, compensated by higher photostability.

■ CONCLUSIONS

The properties and nature of silica gel chromatography make it an ideal support material for organic photocatalysts such as Riboflavin and Eosin. The silica gel particles have a size and

density that allows separation and recovery by simple decantation. In addition, the surface of the Silica gel can be covalently modified by grafting techniques already known for structural derivatives of SiO_2. One aspect that deserves to be improved is the performance of the coupling reactions, since this will reduce the number of dyes used and the number of washes required. Techniques such as TGA and DRS provide quantitative and qualitative information about the hybrid material under study. In addition, visual observation of the material obtained, together with washing cycles and chemical controls, allows confidence that the desired product has been achieved.

Thus, the modified SGs obtained are easy to handle and recover by decantation. Both materials were tested in two singlet oxygen oxidation reactions in two different solvents. In the case of FFA, we could corroborate the consumption of oxygen when the material is irradiated, indicating the formation of singlet oxygen. The photosensitized reaction with DMA in DMF is presented as a proof of concept for use in organic synthesis. Contrary to RF, the higher stability of Eosin Y containing hybrid material can be recovered and reused in several cycles. These results are very encouraging because silica-gel for chromatography is a known material, commercially available and it is widely used in organic chemistry laboratories. We have shown that it is easy to chemically modify and to handle and recover in the laboratory. With appropriate linkers, diverse photosensitizers can be attached to the SG surface. Binding photosensitizers to macroscopic SG allows photochemistry to be applied in a scalable manner. These new materials will make catalyst recovery easier and simplify product purification. This system is environmentally friendly, and its catalytic performance is acceptable.

■ EXPERIMENTAL SECTION

Reagents. All chemical reagents were commercially purchased and used without further purification. Silica gel 60 (0.063−0.200 mm) for column chromatography (70−230 mesh ASTM), and sodium azide (NaN_3), both from Merck, Germany. Succinic anhydride, from Riedel de Haën (AG-D3016 seeize 1). Riboflavin (RF), Eosin Y (Eo), (3-aminopropyl)triethoxysilane (APTES), N,N-dicyclohexylcarbodiimide(DCC), 4-dimethylaminopyridine (DMAP), 9,10-dimethylanthracene (DMA), and furfuryl alcohol (FFA) were all from Sigma, USA.

Solvents: water (miliQ), dichloromethane (DCM), ethyl acetate (EtOAc), and acetone, were distilled before use, while acetic acid, HCl 35% (both p.a ACS, Cicarelli, Argentina) and dimethylsulfoxide (DMSO, p.a ACS, Biopack) N,N-dimethylformamide (DMF, p.a ACS, Biopack) were used as received.

General Equipment: UV−Visible spectra were measured using a Shimadzu 1800 spectrophotometer. FTIR spectra were recorded using a Nicolet iS5 infrared spectrophotometer with ATR iD7 module with ZnSe crystal. Irradiation experiments were carried out in a home-made photoreactor, consisting of 4 vial spots, and 4 LED plates in the bottom. Blue LED 3 W-22 Lm-λ_{max} 455 nm or green LED 3 W-110 Lm-λ_{max} 517 nm.

SG-Succ Preparation. Chromatographic silica gel (SG) was stored in an oven at 100 °C to remove adsorbed moisture that could affect the reactions. A modified version of Martins *et al.* was used for the linker binding.[11] For a typical assay, 2 mmol of succinic anhydride and 1.08 g of SG were placed in 10 mL of refluxing pyridine (120 °C) in a conical flask with

stirring at 90 r.p.m. After 4 h, the reaction was cooled and decanted. Once the product reached the bottom of the vessel, the crude reaction was gently removed with a Pasteur pipette. The recovered solid was subjected to cycles of washing and decanting in the same conical flask. The washings were: 15 mL of 1 M acetic acid in DCM, 15 mL of EtOH 95%, 15 mL of water, 15 mL of 0.1 M HCl, 15 mL of water, and 8 mL and 2 mL of acetone, and finally dried in an oven at 80−100 °C to give 1.01 g of product. This reaction was repeated on a larger scale with 4.38 g of SG, 8 mol of succinic anhydride, and 40 mL of pyridine. SG-Succ formation was established by IR, TGA, and chemical controls of RF covalent attached. Similarly, the assay was repeated using succinic acid as the linker, but in this case, the carbonyl signal was not seen in the IR spectrum, and the final solid was not colored (See SI, Table S2, page S5).

SG-Succ-RF Preparation. For Riboflavin binding, a second reaction was performed based on the work of Neises and Steglich.[34] Several tests were carried out, the final protocol being as follows: First, 5 mL of DCM was cooled in an ice bath in a conical flask. Then 0.2136 g of SG-Succ was taken and reacted with 0.107 mmol (0.0404 g) of RF with 0.113 mmol (0.0234 g) of DCC activator and 1.14 moles (0.1403 g) of DMAP. After 5 min the ice bath was removed, and the reaction was left for 4 h with stirring at 60 r.p.m. After this time, the reaction was then left overnight without stirring. The solution appears orange due to RF and other suspended materials. The following day, the reaction crude containing free RF, DCC, and the diphenyl urea residue was removed. The crude was first washed with the DMF portion, since RF is more soluble in this solvent and then washed several times with water (See SI, page S7). The byproduct diphenyl urea (from DCC) remains on the water, while the modified SG sinks to the bottom of the container. This physical difference allowed us to separate both solid phases in the first water washes. The total amount of 500 mL of water was enough to dissolve the initial amount of RF, which had a solubility value of 84.7 mg/L.[35] Finally, the solid SG-Succ-RF precipitate was washed with ethanol and acetone to clean and dry the product in an oven at 100 °C for 1 h. Each wash was transferred to a volumetric flask for further analysis by UV−visible Spectroscopy. Although the spectroscopic analysis was not accurate enough to quantify the amount of RF bound it was useful to confirm the complete washing of the modified silica, (See SI, page S7). Thus, 0.1785 g of yellow SG-Succ-RF was obtained (84% of the initial mass). FTIR-ATR and DRS studies confirm the presence of RF, and a TGA study indicates that the hybrid material contains 0.035 mmol of RF/gr. This reaction was also tried with DMSO and DMF as solvents, and with EDC as activator, but no colored silica was obtained (See SI, page S9). The assay was repeated several times on a larger scale using 4 g of SG and 0.151 g of RF and equivalent amounts of DCC (0.091 g), DMAP (0.060 g), 70 mL DCM as solvent, and 50 mL each wash with the same solvent sequence.

SG-APTES-Eo Preparation. A conventional grafting technique was used to bind Eosin Y to silica gel with APTES.[8] Briefly, the procedure was as follows: In one vial with 4 mL DMSO, Eosin Y (0.1 mmol) was reacted with APTES (0.21 mmol, 53 μL) and DCC (0.15 mmol in 1 mL DMSO. The reaction was stirred for 2 h in a closed vessel. TLC analysis with AcOEt:hexane 50:50 and 2% EtOH, as mobile phase, showed the formation of a new spot with the same color and fluorescence identified as APTES-Eo with R_f = 0.20, different from the original Eo (R_f = 0.05). The mix APTES-Eo

in DMSO was then transferred to a conical flask containing dry SG in a mixture of 1 mL of pyridine and 1 mL of DMSO under an inert Argon atmosphere. The SG/pyridine premix activates the Si−OH on the surface. An additional 1 mL of DMSO was used to wash the APTES-Eo mix. Finally, the reaction was stirred at 90 r.p.m. for 4 h. The reaction was left overnight without stirring. Then, the reaction crude was gently removed. The decanted pink solid remained at the bottom of the flask. Washes were then made with 2 × 10 mL of DMF, 6 × 50 mL of water, 2 × 25 mL of EtOH, and 10 mL, and 2 mL of acetone. The washings were transferred to a volumetric flask and analyzed by UV−visible spectroscopy. Again, the washes do not allow us to quantify the bound Eo, but they help to ensure the complete removal of the unreacted dye. This reaction was also repeated on a larger scale with 4 g of SG and 0.5 mmol of Eosin Y. In all cases, a pink solid was obtained, which was characterized by TGA, FTIR-ATR, and DRS. These assays indicate the presence of Eosin Y bound to SG.

Thermogravimetric Analysis (TGA). All assays were performed on a TA Instruments Thermogravimeter analyzer (New Castle, DE, USA), Discovery model. The determinations were carried out using an $N_{2(g)}$ flow of 50 mL/min; a heating ramp of 10 °C/min; $T°$ range: 25−800 °C, Pt capsules and sample sizes between 3 and 7 mg. The temperature scale was previously calibrated with nickel according to the protocol recommended by the manufacturer (See SI, page S11).

FTIR-ATR Analysis. Attenuated total reflectance infrared spectra (FT-IR-AR) were performed using Nicolet iS5 equipment with the iD7 ATR accessory and a 45° ZnSe crystal. (Thermo Scientific, USA). All spectra were recorded with 32 scans at a 4 cm^{-1} resolution between 4000 and 550 cm^{-1}. Spectra were processed using OMNIC 9.8.3.32 software from Thermo Fischer Scientific Inc. and with OrginLab Pro 8 SR0 v8.0724 (B724).

Diffuse Reflectance Spectroscopy (DRS). UV−visible diffuse reflectance was measured in UV−Vis Spectrometer Stellar Net using an optical fiber probe and 45° holder for solid samples. With reference to RS50 White Reflectance Standard and dark background. Settings: Absorbance mode, detector integration rate 3000 ms, pixel resolution, pixel smoothing 3 (17), temp compensation on.

Microscopy. Light microscopy was used to observe the morphology and size of commercial or modified silica gel particles. We used a NIKON Eclipse E200LED MV R Microscope, with NIKON CFI E Plan Achromat 4X (0.1/30 mm) and CFI E Plan Achromat 10X (0.25/7 mm) lenses, equipped with a 5.0 Megapixel USB 2.0 Microscope Eyepiece camera. MC500 Camera and software MicroCapture Pro 6.9.12. The grains sample were placed on a glass slide with light from the bottom. A digital camera was used to record ten images per sample. Subsequently, the image collection was analyzed using ImageJ 1.50i software (Wayne Rasband, NHI, USA). Between 800−1200 particles per sample were counted to obtain the population of the different sizes.

DMA Photooxidation. The DMA have 3 intense absorption bands in UV−Vis, and the oxidation product does not absorb in this region. The decrease in absorbance at 379 nm from DMA was used to determine the oxidation process. Depending on the changes in absorbance, the k_{obs} for the *pseudo*-first-order process can be determined. A stock solution of DMA (4.0 ± 0.1) mM in DMF was prepared for the assays. For this, 0.0083 g (4.05 × 10^{-5} mol) of DMA was weighed and dissolved with DMF in a 10 mL flask. Then, 50

μL of this solution was taken and re-dissolved in 4.950 mL of DMF, to get a 40 μM solution with a final volume of 5 mL in a vial (10 mL) with a rubber stopper and a magnetic stirrer. The photosensitizer material was added to this vial. The vial was then stirred and irradiated from the bottom in a photoreactor with a 3 W blue LED for RF or green LED for Eosin Y. After the selected irradiation time, a 3 mL aliquot was collected and transferred to a quartz UV cell; the UV−vis spectrum was then recorded, and finally the entire solution was recovered and re-incorporated into the reaction vial. UV−Visible spectra were recorded at different irradiation times. In all cases, the temperature ranged from room temperature to a maximum of 30 °C at long irradiation times. The DMA photo-sensitization reaction was performed with homogenous RF, SG-Succ-RF, and SG and irradiated with a 445 nm blue LED. For comparison purposes, the amounts of RF in the solution were necessary to obtain an absorbance of 0.3, and for the solid composite 0.0035 g was used, corresponding to an equivalent amount of RF bound to the SG, as calculated by TGA. Similarly, the experiment was performed with homogenous Eosin Y, SG-APTES-Eo, and SG irradiated with a 554 nm green LED. In this case, the amount of SG-APTES-Eo equivalent to eosin 0.3 abs in solution was less than the minimum weighable amount (0.0003 g). In this case, we use the mass of hybrid material equivalent to the SG-Succ-RF assay (0.0038 g). To rule out thermal effects, a control experiment with DMA + SG-Succ-RF was performed in the dark at 36 °C. This control assay shows that the DMA concentration remains unchanged.

Oxygen Uptake Experiments. The ability of the synthesized composite (SG-Succ-RF) to photo generates the reactive singlet oxygen species ($^1O_2$) was studied through O_2-uptake experiments. The O_2-uptake experiments were carried out in a home-made photo-reactor device previously reported.[29] Briefly, this photo-reactor device consists of a 150 W quartz-halogen lamp as an irradiation source, and the O_2-uptake was measured with a selective oxygen electrode (Orion 97-08). All experiments were performed in water at pH 6.0. In a typical experiment, an aqueous suspension of 0.03% w/v SG-Succ-RF was placed in a seated reaction tube. The O_2-uptake experiment was carried out under continuous stirring to ensure the homogeneity of the radiation and to avoid the precipitation of SG-Succ-RF. A similar experiment was done with SG-APTES-Eo. Sensitized photolysis experiments were carried out in the water at pH 6, with a suspension of 0.017% w/v of SG-APTES-Eo plus 500 μM of FFA.

Modified SG Reuse. To test the re-use capabilities of the hybrid SGs, DMA photosensitization cycles were performed. For the assay, 0.1 g of each RF- or Eo-modified silica, was placed in a 10 mL capped vial, and a 3 mL DMA solution of 1.75 mM (5.24 μmol) in DMF as solvent was added. The same 3 W × 4 spot photo-reactor device was used for the blue or green irradiation for RF or Eo, respectively. The vial was irradiated for 1 h with gentle stirring. The vial was then removed from the photoreactor, and the modified SG was allowed to decant. The solution was gently removed and transferred to a quartz cuvette, and the remaining DMA was quantified by UV Visible Spectroscopy (See SI, page S30). The modified SG in the vial was washed with DMF. After removal of the washing DMF, the cycle was repeated. A new 3 mL of 1.75 mM DMA (5.24 μmol) in DMF was then added to the vial, and it is irradiated for 1 h. The DMA consumption (%) in

each cycle was used as an indication of the efficiency of the hybrid material.

ASSOCIATED CONTENT

⬛ Supporting Information

The Supporting Information is available free of charge at https://pubs.acs.org/doi/10.1021/acsomega.3c04622.

> Additional experimental details, comparison of recovery methods and full spectroscopic data (PDF)

AUTHOR INFORMATION

Corresponding Authors

Daniel A. Caminos − *Instituto de Investigaciones en Fisicoquímica de Córdoba, INFIQC, Consejo Nacional de Investigaciones Científicas y Técnicas, CONICET, Ciudad Universitaria, Haya de la Torre y Medina Allende. Ed Cs II. Córdoba, Córdoba X5000HUA, Argentina; Departamento de Química Orgánica, Facultad de Ciencias Químicas, Universidad Nacional de Córdoba, Ciudad Universitaria, Haya de la Torre y Medina Allende. Ed Cs II. Córdoba, Córdoba X5000HUA, Argentina;* orcid.org/0000-0001-7974-7024; Email: dcaminos@unc.edu.ar

Juan E. Argüello − *Instituto de Investigaciones en Fisicoquímica de Córdoba, INFIQC, Consejo Nacional de Investigaciones Científicas y Técnicas, CONICET, Ciudad Universitaria, Haya de la Torre y Medina Allende. Ed Cs II. Córdoba, Córdoba X5000HUA, Argentina; Departamento de Química Orgánica, Facultad de Ciencias Químicas, Universidad Nacional de Córdoba, Ciudad Universitaria, Haya de la Torre y Medina Allende. Ed Cs II. Córdoba, Córdoba X5000HUA, Argentina;* orcid.org/0000-0002-7321-4291; Email: jea@fcq.unc.edu.ar

Authors

Guido N. Rimondino − *Instituto de Investigaciones en Fisicoquímica de Córdoba, INFIQC, Consejo Nacional de Investigaciones Científicas y Técnicas, CONICET, Ciudad Universitaria, Haya de la Torre y Medina Allende. Ed Cs II. Córdoba, Córdoba X5000HUA, Argentina; Departamento de Fisicoquímica, Facultad de Ciencias Químicas, Universidad Nacional de Córdoba, Ciudad Universitaria, Haya de la Torre y Medina Allende. Córdoba, Córdoba X5000HUA, Argentina*

Eduardo Gatica − *Instituto para el Desarrollo Agroindustrial y de la Salud (IDAS). CONICET − UNRC. Depto. de Estudios Básicos y Agropecuarios, Facultad de Agronomía y Veterinaria, Universidad Nacional de Río Cuarto, Rio Cuarto X5804BYA, Argentina*

Walter A. Massad − *Instituto para el Desarrollo Agroindustrial y de la Salud (IDAS), CONICET − UNRC, Depto. de Química − FCEFQyN, Universidad Nacional de Río Cuarto, Rio Cuarto X5804BYA, Argentina*

Complete contact information is available at:
https://pubs.acs.org/10.1021/acsomega.3c04622

Notes

The authors declare no competing financial interest.
D.A.C.: Conceptualization, experiments, and manuscript redaction. G.N.R.: FTIR-ATR assays and analysis. E.G.: Oxygen uptake measurements. W.A.M.: Conceptualization of singlet oxygen experiments and analysis. J.E.A.: Conceptualization, manuscript redaction, and funding.

REFERENCES

(1) *Sustainable Industrial Chemistry: Principles, Tools, and Industrial Examples*; Cavani, F., Centi, G., Perathoner, S., Trifiro, F., Eds.; Wiley-VHC: Weinheim, 2009.

(2) (a) Xiea, J.; Jina, H.; Xua, P.; Zhu, C. When C−H bond functionalization meets visible-light photoredox catalysis. *Tetrahedron Lett.* **2014**, *55*, 36−48. (b) Hari, D. P.; König, B. Synthetic applications of eosin Y in photoredox catalysis. *Chem. Commun.* **2014**, *50*, 6688−6699. (c) Prier, C. K.; Rankic, D. A.; MacMillan, D. W. C. Visible Light Photoredox Catalysis with Transition Metal Complexes: Applications in Organic Synthesis. *Chem. Rev.* **2013**, *113*, 5322−5363. (d) Hari, D. P.; Hering, T.; König, B. The Photoredox-Catalyzed Meerwein Addition Reaction: Intermolecular Amino-Arylation of Alkenes. *Angew. Chem., Int. Ed.* **2014**, *53*, 725−728. (e) Narayanam, J. M. R.; Stephenson, C. R. J. Visible light photodevice catalysis: applications in organic synthesis. *Chem. Soc. Rev.* **2011**, *40*, 102−113. (f) Ischay, M. A.; Yoon, T. P. Accessing the Synthetic Chemistry of Radical Ions. *Eur. J. Org. Chem.* **2012**, 3359−3372.

(3) Sharma, S.; Sharma, A. Recent advances in photocatalytic manipulations of Rose Bengal in organic synthesis. *Org. Biomol. Chem.* **2019**, *17*, 4384−4405.

(4) (a) Ravelli, D.; Fagnoni, M.; Albini, A. Photoorganocatalysis. What for? *Chem. Soc. Rev.* **2013**, *42*, 97−113. (b) Xi, Y.; Yi, H.; Lei, A. Synthetic applications of photoredox catalysis with visible light. *Org. Biomol. Chem.* **2013**, *11*, 2387−2403.

(5) (a) Du, Y.; Pearson, R. M.; Lim, C.-H.; Sartor, S. M.; Ryan, M. D.; Yang, H.; Damrauer, N. H.; Miyake, G. M. Strongly Reducing, Visible-Light Organic Photoredox Catalysts as Sustainable Alternatives to Precious Metals. *Chem. — Eur. J.* **2017**, *23*, 10962−10968. (b) Nicewicz, D. A.; Nguyen, T. M. Recent Applications of Organic Dyes as Photoredox Catalysts in Organic Synthesis. *ACS Catal.* **2014**, *4*, 355−360. (c) Romero, N. A.; Nicewicz, D. A. Organic Photoredox Catalysis. *Chem. Rev.* **2016**, *116*, 10075−10166.

(6) (a) Bouchet, L. M.; Peñéñory, A. B.; Argüello, J. E. Synthesis of arylselenide ethers by photoinduced reactions of selenobenzamide, selenourea and selenocyanate anions with aryl halides. *Tetrahedron Lett.* **2011**, *52*, 969−972. (b) Argüello, J. E.; Schmidt, L. C.; Peñéñory, A. B. "One-Pot" Two-Step Synthesis of Aryl Sulfur Compounds by Photoinduced Reactions of Thiourea Anion with Aryl Halides. *Org. Lett.* **2003**, *5*, 4133−4136. (c) Schmidt, L. C.; Rey, V.; Peñéñory, A. B. Photoinduced Nucleophilic Substitution of Aryl Halides with Potassium Thioacetate—A One-Pot Approach to Aryl Methyl and Diaryl Sulfides. *Eur. J. Org. Chem.* **2006**, 2210−2214. (d) Schmidt, L. C.; Argüello, J. E.; Peñéñory, A. B. Nature of the Chain Propagation in the Photostimulated Reaction of 1-Bromonaphthalene with Sulfur-Centered Nucleophiles. *J. Org. Chem.* **2007**, *72*, 2936−2944. (e) Oksdath-Mansilla, G.; Argüello, J. E.; Peñéñory, A. B. Photoreduction of aliphatic and aromatic thioketals: new access to the reduction of carbonyl groups by a desulfurization chain process. *Tetrahedron Lett.* **2013**, *54*, 1515−1518. (f) Argüello, J. E.; Pérez-Ruiz, R.; Miranda, M. A. Novel [4+2] cycloaddition between thiobenzophenone and aryl-substituted alkenes via photoinduced electron transfer. *Org. Lett.* **2007**, *9*, 3587−3590. (g) Oksdath-Mansilla, G.; Hajj, V.; Andrada, D. M.; Argüello, J. E.; Bonin, J.; Robert, M.; Peñéñory, A. B. Peñéñory, Photoremoval of Protecting Groups: Mechanistic Aspects of 1,3-Dithiane Conversion to a Carbonyl Group. *J. Org. Chem.* **2015**, *80*, 2733−2739. (h) Castro-

Godoy, W. D.; Heredia, A. A.; Schmidt, L. C.; Argüello, J. E. A straightforward and sustainable synthesis of 1,4-disubstituted 1,2,3-triazoles via visible-light-promoted copper-catalyzed azide−alkyne cycloaddition (CuAAC). *RSC Adv.* **2017**, *7*, 33967−33973. (i) Bouchet, L. M.; Argüello, J. E. Photoinduced One-Electron Oxidation of Aromatic Selenides: Effect of the Structure on the Reversible Dimerization Reaction. *J. Org. Chem.* **2018**, *83*, 5674−5680. (j) Lemir, I. D.; Argüello, J. E.; Lanterna, A. E.; Scaiano, J. C. Heterogeneous photocatalysis of azides: extending nitrene photochemistry to longer wavelengths. *Chem. Commun.* **2020**, *56*, 10239−10242.

(7) (a) Metternich, J. B.; Sagebiel, S.; Lückener, A.; Lamping, S.; Ravoo, B. J.; Gilmour, R. Covalent Immobilization of (−)-Riboflavin on Polymer Functionalized Silica Particles: Application in the Photocatalytic E→Z Isomerization of Polarized Alkenes. *Chem. − Eur. J.* **2018**, *24*, 4228−4233. (b) Jessica, Š.; Eva, S.; Tomáš, H.; Ivan, S.; Jitka, K.; Jana, C.; Josef, C.; Radek, C. Visible Light [2+2] Photocycloaddition Mediated by Flavin Derivative Immobilized on Mesoporous Silica. *ChemCatChem* **2017**, *9*, 1177−1181. (c) Kumar, G.; Solanki, P.; Nazish, M.; Neogi, S.; Kureshy, R. I.; Khan, N.-u. H. Covalently hooked EOSIN-Y in a Zr(IV) framework as visible-light mediated, heterogeneous photocatalyst for efficient CH functionalization of tertiary amines. *J. Catal.* **2019**, *371*, 298−304.

(8) Guo, S.; Zhang, H.; Huang, L.; Guo, Z.; Xiong, G.; Zhao, J. Porous material-immobilized iodo-Bodipy as an efficient photocatalyst for photoredox catalytic organic reaction to prepare pyrrolo[2,1-a]isoquinoline. *Chem. Commun.* **2013**, *19*, 8689.

(9) Ferrari, G. V.; Andrada, M. E.; Natera, J.; Muñoz, V. A.; Montaña, M. P.; Gambetta, C.; Boiero, M. L.; Montenegro, M. A.; Massad, W. A. *Photochem. Photobiol.* **2014**, *90*, 1251−1256.

(10) (a) McKenzie, T. G.; Fu, Q.; Wong, E. H. H.; Dunstan, D. E.; Qiao, G. G. *Macromolecules* **2015**, *48*, 3864−3872. (b) Xiangyong, G.; Li, X.; Chai, Y.; Yang, Q.; Li, P.; Yao, Y. *Green Chem.* **2013**, *15*, 357−361. (c) Xie, Z.; Wang, C.; deKrafft, K. E.; Lin, W. *J. Am. Chem. Soc.* **2011**, *133*, 2056−2059. (d) Zwijnenburg, M. A.; Cheng, G.; McDonald, T. O.; Jelfs, K. E.; Jiang, J.-X.; Ren, S.; Hasell, T.; Blanc, F.; Cooper, A. I.; Adams, D. J. *Macromolecules* **2013**, *46*, 7696−7704. (e) Sun, Q.; Dai, Z.; Meng, X.; Xiao, F.-S. *Chem. Soc. Rev.* **2015**, *44*, 6018. (f) Wang, C.-A.; Li, Y.-W.; Cheng, X.-L.; Zhang, J.-P.; Han, Y.-F. Eosin Y dye-based porous organic polymers for highly efficient heterogeneous photocatalytic dehydrogenative coupling reaction. *RSC Adv.* **2017**, *7*, 408−414.

(11) (a) Zhang, T.; Liang, W.; Huang, Y.; Li, X.; Liu, Y.; Yang, B.; He, C.; Zhou, X.; Zhang, J. *Chem. Commun.* **2017**, *53*, 12536−12539. (b) Li, X.; Li, Y.; Huang, Y.; Zhang, T.; Liu, Y.; Yang, B.; He, C.; Zhou, X.; Zhang, J. *Green Chem.* **2017**, *19*, 2925−2930.

(12) Martins, L. R.; Baêta, B. E. L.; Alves Gurgel, L. V.; de Aquino, S. F.; Gil, L. F. Application of cellulose-immobilized riboflavin as a redox mediator for anaerobic degradation of a model azo dye Remazol Golden Yellow RNL. *Ind. Crops Prod.* **2015**, *65*, 454−462.

(13) Xiao, L.; Huang, Y.; Luo, Y.; Yang, B.; Liu, Y.; Zhou, X.; Zhang, J. Organic Cotton Photocatalysis. *ACS Sustainable Chem. Eng.* **2018**, *6*, 14759−14766.

(14) Ribeiro, S. M.; Serra, A. C.; Rocha Gonsalves, A. M. d.' A. Immobilised porphyrins in monoterpene photooxidations. *J. Catal.* **2008**, *256*, 331−337.

(15) (a) Sridhar, A.; Rangasamy, R.; Selvaraj, M. Polymer-supported eosin Y as a reusable photocatalyst for visible light mediated organic transformations. *New J. Chem.* **2019**, *43*, 17974−17979. (b) Li, P.; Wang, G.-W.; Zhu, X.; Wang, L. Magnetic nanoparticle-supported eosin Y ammonium salt: An efficient heterogeneous catalyst for visible light oxidative C−C and C−P bond formation. *Tetrahedron* **2019**, *75*, 3448−3455.

(16) Schmaderer, H.; Hilgers, P.; Lechner, R.; König, B. Photooxidation of Benzyl Alcohols with Immobilized Flavins. *Adv. Synth. Catal.* **2009**, *351*, 163−174.

(17) Hao, H.; Li, X.; Lang, X. Anthraquinones as photoredox active ligands of TiO$_2$ for selective aerobic oxidation of organic sulfides. *Appl. Catal., B* **2019**, *259*, No. 118038.

(18) Jiménez-Hernández, M. E.; Manjón, F.; García-Fresnadillo, D.; Orellana, G. Solar water disinfection by singlet oxygen photogenerated with polymer-supported Ru(II) sensitizers. *Sol. Energy* **2006**, *80*, 1382−1387.

(19) Dongare, P.; MacKenzie, I.; Wang, D.; Nicewicz, D. A.; Meyer, T. J. Oxidation of alkyl benzenes by a flavin photooxidation catalyst on nanostructured metal-oxide films. *Proc. Natl. Acad. Sci. U. S. A.* **2017**, *114*, 9279−9283.

(20) Cabezuelo, O.; Martinez-Haya, R.; Montes, N.; Bosca, F.; Marin, M. L. Heterogeneous riboflavin-based photocatalyst for pollutant oxidation through electron transfer processes. *Appl. Catal., B* **2021**, *298*, No. 120497.

(21) Shibata, K.; Kiyoura, T.; Hayashi, Y. Acid property and catalytic activity of silica gel treated with ammonium salts. *J. Res. Inst. Catal. Hokkaido Univ.* **1971**, *19*, 29−34. available in http://hdl.handle.net/2115/24918, (access Nov 2022).

(22) Srivastava, V.; Singh, P. K.; Srivastava, A.; Singh, P. P. Synthetic applications of flavin photocatalysis: a review. *RSC Adv.* **2021**, *11*, 14251−14259.

(23) Srivastava, V.; Singh, P. P. Eosin Y catalysed photoredox synthesis: a review. *RSC Adv.* **2017**, *7*, 31377.

(24) Millipore SDS Silica gel 60 (0.063−0.200 mm) for column chromatography (70−230 mesh ASTM) merck (https://www.sigmaaldrich.com/AR/en/sds/mm/1.07734, (access Nov 2022).

(25) Kumano, D.; Iwahana, S.; Iida, H.; Shen, C.; Crassous, J.; Yashima, E. Enantio separation on Riboflavin Derivatives Chemically Bonded to Silica Gel as Chiral Stationary Phases for HPLC. *Chirality* **2015**, *27*, 507−517.

(26) Rosa-Pardo, I.; Roig-Pons, M.; Heredia, A. A.; Usagre, J. V.; Ribera, A.; Galian, R. E.; Pérez-Prieto, J. Fe$_3$O$_4$@Au@mSiO$_2$ as an enhancing nanoplatform for Rose Bengal photodynamic activity. *Nanoscale* **2017**, *9*, 10388−10396.

(27) Fernandes, A. E.; Jonas, A. M. Design and engineering of multifunctional silica-supported cooperative catalysts. *Catal. Today* **2019**, *334*, 173−186.

(28) Gambetta, C.; Massad, W. A.; Nesci, A. V.; García, N. A. Vitamin B2-sensitized degradation of the multifunctional drug Evernyl, in the presence of visible light − microbiological implications. *Pure Appl. Chem.* **2015**, *87*, 997−1010.

(29) Haag, W. R.; Hoigné, J.; Gassman, E.; Braun, A. Singlet oxygen in surface waters — Part I: Furfuryl alcohol as a trapping agent. *Chemosphere* **1984**, *13*, 631−640.

(30) Scully, F. E.; Hoigné, J. Rate constants for reactions of singlet oxygen with phenols and other compounds in water. *Chemosphere* **1987**, *16*, 681−694.

(31) Burns, J. M.; Cooper, W. J.; Ferry, J. L.; King, D. W.; DiMento, B. P.; McNeill, K.; Miller, C. J.; Miller, W. L.; Peake, B. M.; Rusak, S. A.; Rose, A. L.; Waite, T. D. Methods for reactive oxygen species (ROS) detection in aqueous environments. *Aquat. Sci.* **2012**, *74*, 683−734.

(32) Wilkinson, F.; Helman, W. P.; Ross, A. B. Rate constants for the decay and reactions of the lowest electronically excited singlet state of molecular oxygen in solution. An expanded and revised compilation. *J. Phys. Chem. Ref. Data* **1995**, *24*, 663−677.

(33) Martínez-Haya, R.; Heredia, A. A.; Castro-Godoy, W. D.; Schmidt, L. C.; Marin, M. L.; Argüello, J. E. Mechanistic Insight into the Light-Triggered CuAAC Reaction: Does Any of the Photocatalyst Go? *J. Org. Chem.* **2021**, *86*, 5832−5844.

(34) Neises, B.; Steglich, W. Simple Method for the Esterification of Carboxylic Acids. *Angew. Chem., Int. Ed.* **1978**, *17*, 522−524.

(35) Riboflavin, Compound summary, *Pub Chem*, National Library of Medicine, web site https://pubchem.ncbi.nlm.nih.gov/compound/Riboflavin, (access 11, **2022**).